NANO LETTERS
Cite This: Nano Lett. 2020, 20, 1089−1100
Letter
pubs.acs.org/NanoLett

Sonogenetic Modulation of Cellular Activities Using an Engineered Auditory-Sensing Protein

Yao-Shen Huang,[†] Ching-Hsiang Fan,[‡] Ning Hsu,[†] Nai-Hua Chiu,[‡] Chun-Yao Wu,[‡] Chu-Yuan Chang,[†] Bing-Huan Wu,[†] Shi-Rong Hong,[†] Ya-Chu Chang,[†] Anthony Yan-Tang Wu,[§,∥,⊥] Vanessa Guo,[§] Yueh-Chen Chiang,[†] Wei-Chia Hsu,[†] Linyi Chen,[†,#] Charles Pin-Kuang Lai,[§,∥,▽] Chih-Kuang Yeh,[*,‡] and Yu-Chun Lin[*,†,#]

[†]Institute of Molecular Medicine, National Tsing Hua University, Hsinchu 300, Taiwan
[‡]Department of Biomedical Engineering and Environmental Sciences, National Tsing Hua University, Hsinchu 300, Taiwan
[§]Institute of Atomic and Molecular Sciences, Academia Sinica, Taipei 106, Taiwan
[∥]Chemical Biology and Molecular Biophysics Program, Taiwan International Graduate Program, Academia Sinica, Taipei 106, Taiwan
[⊥]Department and Graduate Institute of Pharmacology, National Taiwan University, Taipei 106, Taiwan
[#]Department of Medical Science, National Tsing Hua University, Hsinchu 300, Taiwan
[▽]Genome and Systems Biology Degree Program, National Taiwan University and Academia Sinica, Taipei 106, Taiwan

Supporting Information

ABSTRACT: Biomolecules that respond to different external stimuli enable the remote control of genetically modified cells. We report herein a sonogenetic approach that can manipulate target cell activities by focused ultrasound stimulation. This system requires an ultrasound-responsive protein derived from an engineered auditory-sensing protein prestin. Heterologous expression of mouse prestin containing two parallel amino acid substitutions, N7T and N308S, that frequently exist in prestins from echolocating species endowed transfected mammalian cells with the ability to sense ultrasound. An ultrasound pulse of low frequency and low pressure efficiently evoked cellular calcium responses after transfecting with prestin(N7T, N308S). Moreover, pulsed ultrasound can also noninvasively stimulate target neurons expressing prestin(N7T, N308S) in deep regions of mouse brains. Our study delineates how an engineered auditory-sensing protein can cause mammalian cells to sense ultrasound stimulation. Moreover, our sonogenetic tools will serve as new strategies for noninvasive therapy in deep tissues.

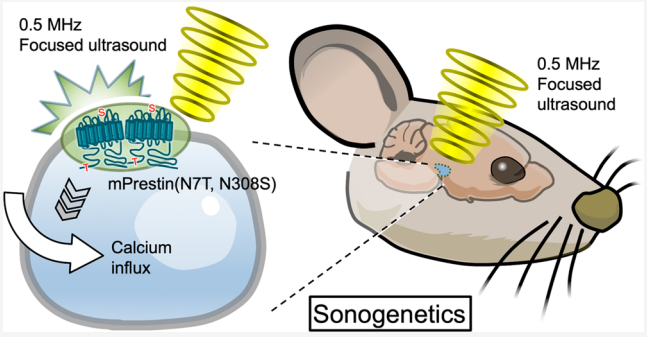

KEYWORDS: *Sonogenetics, focused ultrasound, mammalian cells, neuromodulation*

Approaches that can noninvasively stimulate target cells buried in the deep tissues are highly desirable for basic research and clinical therapy. Currently, different external stimuli including photons, chemicals, radio waves, and magnetic fields have been used to stimulate target cells implanted with stimulus-responsive proteins or nanoparticles.[1−4] However, these strategies suffer from several drawbacks including invasiveness, poor spatiotemporal precision, or low penetration depth, which greatly hinder their potential use in clinical therapy. To overcome these long-standing problems, we aim to use focused ultrasound (FUS) as a stimulus to remotely control cellular activities because it can noninvasively deliver acoustic energy to deep tissues while retaining spatiotemporal coherence.[5]

Ultrasound waves have frequencies greater than those of sound waves that can be heard by humans (>20 kHz). Low-frequency ultrasound waves (<3.5 MHz) are easily transmitted through tissues, including those of bones and brains.[6] Owing to its deep penetrability and spatiotemporal resolution (a few cubic millimeters), ultrasound-based neuromodulation has been tested on cultured neuronal cells and in brains of various model organisms.[6−11] As continuous ultrasound waves or pulsed ultrasound waves of high acoustic pressure are typically needed to activate neurons, neuronal cells are likely to be weakly sensitive to ultrasound stimulus.[8,12,13] To overcome this, gas-filled microbubbles (MBs) that vibrate upon ultrasound excitation have been used as ultrasound amplifiers to

Received: October 23, 2019
Revised: December 23, 2019
Published: December 29, 2019

DOI: 10.1021/acs.nanolett.9b04373
Nano Lett. 2020, 20, 1089−1100

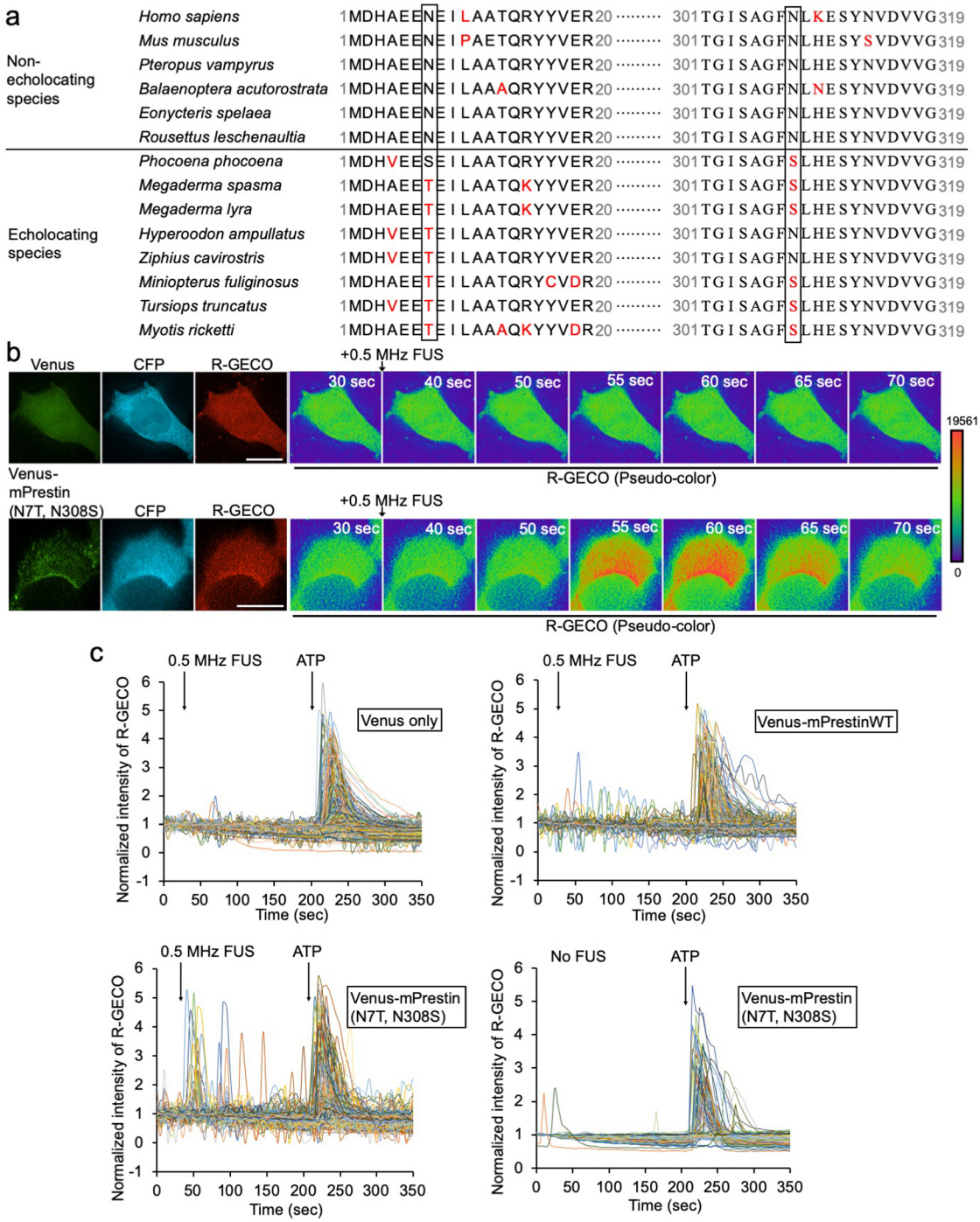

Figure 1. mPrestin carrying the N7T and N308S mutations functions as an ultrasound-responsive protein. (a) Sequence alignment of prestins from six nonecholocating and eight echolocating species showing that N7T and N308S substitutions frequently occurred in the echolocating species. Positions 7 and 308 are boxed with the residues located at those positions highlighted in red. (b) Excitation of 0.5 MHz FUS evokes calcium responses in cells expressing Venus-mPrestin(N7T, N308S) but not in control cells expressing Venus alone. Cells were cotransfected with the calcium biosensor CFP-R-GECO. The intensity of the R-GECO fluorescence in the cells was monitored by live-cell imaging. Scale bar, 10 μm. (c) Time course of R-GECO fluorescence intensity in cells expressing the indicated constructs in the presence or absence of 0.5 MHz FUS stimulation. ATP treatment (10 μM) served as a positive control to show that the cells could exhibit intracellular calcium flux. Data were collected for 7−36 independent experiments, with n = 250 cells per experiment.

enhance their mechanical effects on target cells.[14,15] Recently, Ibsen and colleagues used MBs to transduce mechanical stimulation from ultrasound waves to neuronal cells in *Caenorhabditis elegans* and induced behavioral output.[16] The pore-forming cationic mechanotransduction ion channel TRP-4 may be involved in transducing ultrasound stimulation onto MBs attached to *Caenorhabditis elegans*.[16] Although this study verified that ultrasound-mediated neuromodulation is possible, its further development faces major roadblocks; i.e., MBs have a short lifespan *in vivo* (<5 min in the blood), and it is difficult to deliver MBs to extravascular tissues.[17] Compared with MBs, gas-filled protein complexes, denoted as gas vesicles, are highly

DOI: 10.1021/acs.nanolett.9b04373
Nano Lett. 2020, 20, 1089−1100

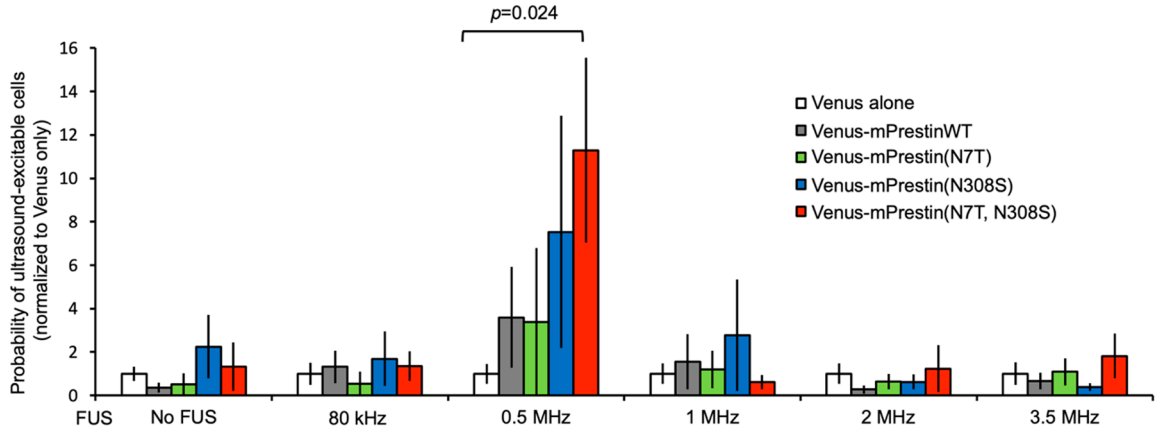

Figure 2. mPrestin(N7T, N308S) enables an ultrasound-evoked calcium response in a frequency-specific manner. HEK293T cells transfected with one of the indicated DNA constructs were bathed in PBS and stimulated with ultrasound of different frequencies (3 s duration, 2000 cycles, 10 Hz PRF, 0.5 MPa). Data are presented as the relative percentage of cells in each group (expressed as fold-probability) that were excitable by ultrasound after normalization to that of cells expressing only Venus that were stimulated at the same frequency. The cells whose R-GECO intensity increases more than 1.2-fold over resting value after ultrasound stimulation were defined as ultrasound-excitable cells. The cells with small or no increase in R-GECO intensity (<1.2-fold) were defined as ultrasound-unexcitable cells. The absolute number of cells in each group was 998, 556, 686, 739, 780, 3111, 438, 277, 691, 1484, 1515, 408, 472, 785, 771, 1735, 856, 1571, 1085, 520, 1470, 1050, 1250, 1199, and 605 cells from left to right. Data are shown as the mean ± s.e.m. for 7−36 independent experiments. *P*-values >0.05 are not shown.

stable both *in vitro* and *in vivo* and efficiently oscillate in response to ultrasound excitation. Different gas vesicle variants can serve as genetically encoded ultrasound contrast reagents to track target microbes or cells by ultrasound imaging.[18,19] However, it is still challenging to express and assemble prokaryotic gas vesicles in mammalian cells.[5] Recently, several groups implanted mechanosensitive ion channels, such as Mscl and Piezo1, into *in vitro* cell culture systems and, with their use, successfully perturbed the cellular membrane potentials of target cells using ultrasound.[20,21] However, the ultrasound frequencies used in those studies are too high (30 and 43 MHz) to be applicable for *in vivo* use owing to their low penetrability (<5 mm). Therefore, to date, there has been no sonogenetic system that uses low-frequency and low-pressure ultrasound to remotely control activities of mammalian cells that have been genetically modified.

Several mammalian species, including bats and cetaceans, use ultrasound to navigate or communicate. The high-frequency auditory sensitivity and selectivity in echolocating mammals have been attributed to adaptive mechanical amplification in the outer hair cells (OHCs) of their cochlea.[22] Prestin (also known as SCL26A5) is a transmembrane protein residing in OHCs that drives their electromotility and seems to be involved in the ability to hear ultrasound.[23−25] Heterologous expression of prestin endows transfected mammalian cell lines with several of the physiological hallmarks of OHCs, indicating that prestin inherently acts as an electromechanical transducer.[26] The evolutionary analysis also suggests that prestin is involved in ultrasound sensing of echolocating mammals.[23] The primary sequence of prestin is largely conserved among various mammalian species, although several specific amino acid substitutions that directly affect the electromotility capacity of prestin frequently occur in prestins of sonar mammals but not in those of their nonsonar counterparts.[23,24] Thus, prestin probably enhances ultrasound sensitivity in mammals, although how it does so is still unclear. In this study, we aimed to test the possibility of using prestins with different amino acid substitutions to increase the ultrasound excitability of mammalian cells.

Here, we first examined the amino acid sequences of prestin from six nonecholocating species and eight echolocating species. Asparagine (Asn) at positions 7 and 308 in prestins of nonecholocating species is frequently replaced with threonine (Thr) and serine (Ser), respectively, in echolocating species (Figure 1a). To test whether these apparently evolutionarily driven amino acid substitutions are important to adaptive ultrasound sensing, two mutations N7T and/or N308S were introduced into mouse prestin (hereafter mPrestin). The constructs used for our study were wild-type prestin (mPrestinWT); mPrestin mutants containing a single substitution, mPrestin(N7T) and mPrestin(N308S); and a mutant containing two substitutions, mPrestin(N7T, N308S). These constructs were tagged with the yellow fluorescent protein Venus. Each construct was cotransfected with the calcium biosensor cyan fluorescent protein (CFP)-R-GECO into the human HEK293T cell line. The calcium influx of transfected cells was used as a readout in response to the mechanical stimulation of the ultrasound wave. The reason we chose to measure calcium influx is that ultrasound induces calcium influx of cells in the presence of different nanoparticles.[15,27,28] To simultaneously excite FUS and acquire real-time cell images, an ultrasound transducer connected to a waveform generator and an amplifier was placed on top of the live-cell imaging system. This system focuses ultrasound waves to a circle with a diameter of a few millimeters over a monolayer of cultured cells (Figures S1 and S2). Using this ultrasound-imaging system, we stimulated cells coexpressing CFP-R-GECO and Venus-mPrestin(N7T, N308S) or coexpressing CFP-R-GECO and Venus with a short, low-frequency ultrasound pulse (0.5 MHz, all pulses consisted of 3 s duration, 2000 cycles, 10 Hz of pulse repetition frequency (PRF), 0.5 MPa unless otherwise noted). Live-cell imaging showed that a short ultrasound pulse of 0.5 MHz was sufficient to evoke calcium influx in cells expressing Venus-mPrestin(N7T, N308S), but not in cells transfected with Venus alone (Figure 1b and Movie S1). Quantification of the calcium imaging data indicated that FUS induced a 351 ± 20% (mean ± s.e.m.) increase in the R-GECO fluorescence of Venus-mPrestin(N7T,

DOI: 10.1021/acs.nanolett.9b04373
Nano Lett. 2020, 20, 1089−1100

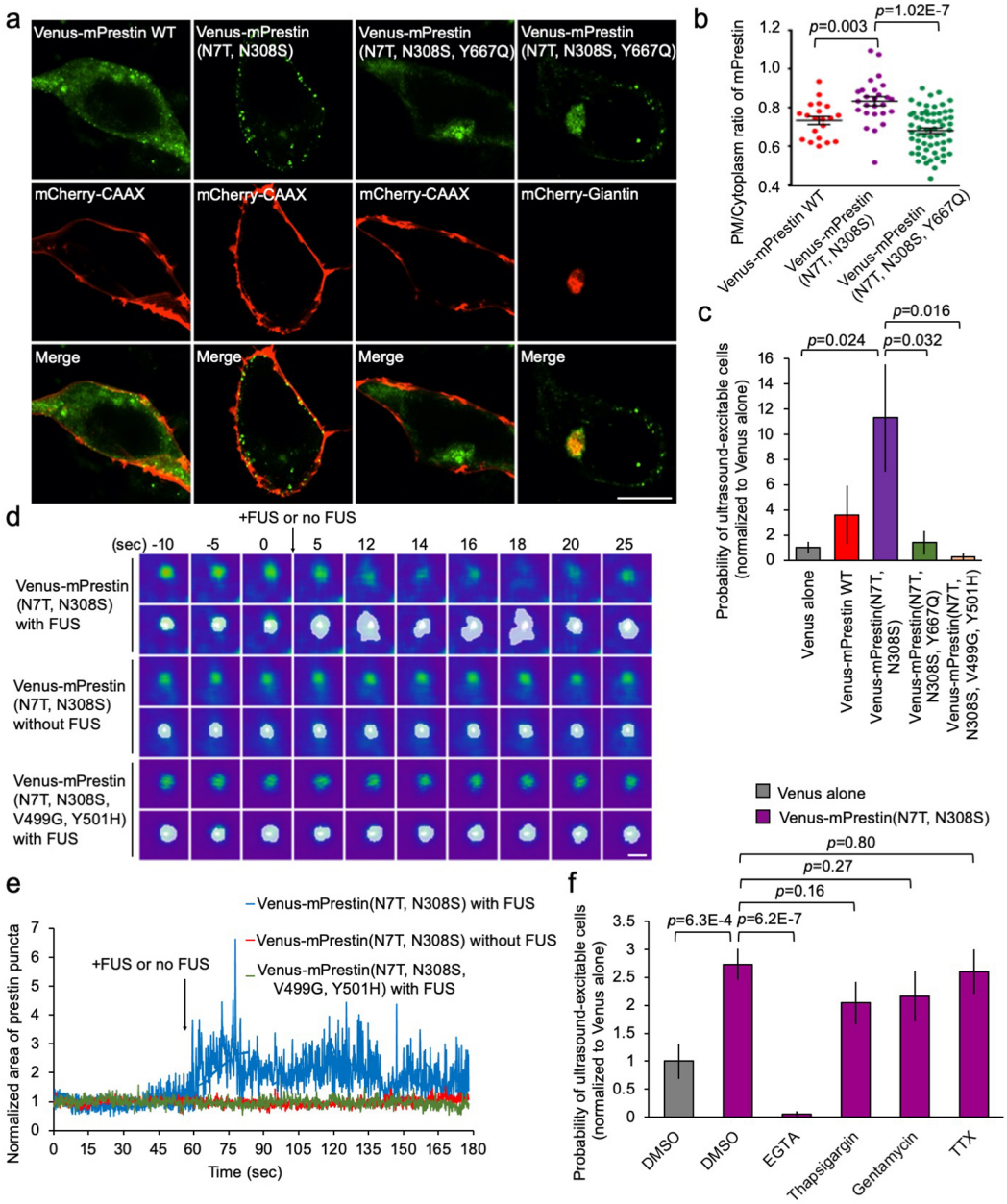

Figure 3. mPrestin(N7T, N308S) puncta oscillate upon FUS stimulation and trigger calcium influx from the extracellular pool. (a) Representative confocal images of HEK293T cells expressing Venus-mPrestinWT, Venus-mPrestin(N7T, N308S), mCherry-CAAX (a plasma membrane marker), or mCherry-Giantin (a Golgi marker). For each field, the maximum *z*-projection was created from 15 stacks, each separated by 0.3 μm. Scale bar, 10 μm. (b) Quantification of the plasma membrane/cytoplasm ratio for the indicated mPrestin constructs. Data are shown as the mean ± s.e.m. for three independent experiments; n = 22, 26, and 61 cells from left to right. (c) HEK293T cells expressing the indicated constructs were stimulated with 0.5 MHz FUS (3 s duration, 2000 cycles, 10 Hz PRF, 0.5 MPa). Data are presented as in Figure 2. The absolute number of cells in each group was 3111, 438, 1484, 532, and 430 cells from left to right. The data are shown as the mean ± s.e.m. for 6−36 independent experiments. (d) Video frames showing the structural dynamics of mPrestin-positive puncta in cells that had or had not been stimulated with 0.5 MHz FUS. The boundaries of the punctate regions are outlined in white. Scale bar, 0.2 μm. (e) Area measurements of mPrestin-positive puncta with or without FUS stimulation. (f) HEK293T cells expressing Venus-mPrestin(N7T, N308S) were incubated with EGTA (5 mM, 20 min), thapsigargin (100 nM, 30 min), gentamycin (200 μM, 20 min), or TTX (500 nM, 20 min) in DMEM and were stimulated with 0.5 MHz FUS (3 s duration, 2000 cycles, 10 Hz PRF, 0.5 MPa); 0.1% DMSO served as the control. Data are presented as in Figure 1b. The absolute number of cells in each group was 1642, 1238, 1826, 1996, 566, and 772 from left to right. Data are shown as the mean ± s.e.m. for 6−12 independent experiments.

N308S)-transfected cells (Figure 1c). However, FUS only slightly evoked the calcium response in cells that expressed Venus-mPrestinWT (Figure 1c). Cells transfected with Venus alone did not respond to FUS stimulation (Figure 1c). Moreover, expression of Venus-mPrestin(N7T, N308S) did not induce spontaneous calcium response in the absence of FUS stimulation (Figure 1c). These results indicated that heterologous expression of Venus-mPrestinWT endowed the transfected cells with a weak ability to sense ultrasound. Substituting Thr at position 7 and Ser at position 308 in the Venus-tagged mPrestinWT substantially improved the ultra-

DOI: 10.1021/acs.nanolett.9b04373
Nano Lett. 2020, 20, 1089−1100

sound-evoked calcium response of the transfected HEK293T cells.

To determine the optimal ultrasound frequency/frequencies for cell manipulation, we next comprehensively tested the calcium responses of cells expressing the various Venus-mPrestin constructs to different FUS frequencies between 80 kHz and 3.5 MHz (3 s duration, 2000 cycles, 10 Hz PRF, 0.5 MPa; Figure 2). Five different ultrasound transducers were utilized to deliver ultrasound waves at various frequencies to mPrestin-transfected cells (Table S1). The power density of US at different frequencies applied to cells was similar (16.4−26.7 mW/cm^2; Table S2). Interestingly, cells individually expressing the WT and mutated constructs were sensitive only to 0.5 MHz FUS (Figure 2). The 80 kHz, 1, 2, and 3.5 MHz FUS were insufficient to evoke a calcium influx in the cells (Figure 2). Moreover, expression of various mPrestin proteins did not induce spontaneous calcium responses in the absence of FUS stimulation (Figure 2). Upon stimulation by 0.5 MHz FUS, the percentage of ultrasound-responsive cells was 11.29 ± 4.25-fold (mean ± s.e.m.) greater for the Venus-mPrestin-(N7T, N308S) group compared with the control group (p = 0.024; Figure 2). Heterologous expression of Venus-mPrestinWT, Venus-mPrestin(N7T), and Venus-mPrestin-(N308S) only slightly increased the sensitivity of the transfected HEK293T cells to 0.5 MHz FUS (p = 0.31, 0.51, and 0.25, respectively; Figure 2). Moreover, the parameter of FUS excitation we used does not affect cell viability or cell membrane integrity (Figures S3 and S4). These results confirmed that 0.5 MHz FUS efficiently evoked a calcium response in cells expressing mPrestin(N7T, N308S) in a frequency-dependent manner.

In addition to prestin, Ibsen and colleagues demonstrated that the mechanosensitive ion channel, TRP-4, is required for ultrasound-mediated mechanical stimulation and can modify animal behavior in the presence of MBs.[16] To test whether TRP-4 can act as an ultrasound-responsive protein, we transfected HEK293T cells with two members of the mammalian TRPC4 family including human TRPC4α (hTRPC4α) and mouse TRPC4β (mTRPC4β).[29,30] The calcium response of cells expressing hTRPC4α or mTRPC4β tagged with CFP upon FUS stimulation of different frequencies was examined and quantified. The percentage of ultrasound-excitable cells in the mTRPC4β-CFP group was 3.29 ± 0.94-fold (mean ± s.e.m.) greater than the control group upon stimulation with 0.5 MHz FUS (p = 0.044; Figure S5). Ultrasound of 80 kHz, 1, 2, and 3.5 MHz was not sufficient to induce a calcium response in cells expressing mTRPC4β-CFP. Thus, mTRPC4β-CFP is only weakly sensitive to 0.5 MHz FUS. Although its protein sequence is very similar to that of mTRPC4β, hTRPC4α-CFP did not respond to the low-frequency ultrasound stimulation at all (Figure S5). Taken together, the comprehensive examination of ultrasound sensing in cells transfected with different putative ultrasound-responsive proteins shows that mPrestin(N7T, N308S) was the most responsive protein.

We next explored the possible molecular mechanisms that make the two evolutionarily conserved amino acid substitutions important for prestin-dependent ultrasound sensing. Targeting of prestin to the plasma membrane is required for its function.[31] Confocal images of Venus-mPrestinWT and Venus-mPrestin(N7T, N308S) in living cells showed that Venus-mPrestinWT localized to the cytoplasm and to the plasma membrane, whereas Venus-mPrestin(N7T, N308S) more frequently localized to the plasma membrane (Figure 3a). Quantification of the relative intensities confirmed that mPrestin(N7T, N308S) exhibited a significantly greater plasma membrane/cytoplasm intensity ratio than did Venus-mPrestinWT (p = 0.003; Figure 3b). We therefore hypothesized that targeting mPrestin(N7T, N308S) to the plasma membrane is important for its sensitivity to ultrasound. To assess this hypothesis, we introduced a point mutation (Y667Q) that causes prestin to mislocate to the Golgi apparatus into Venus-mPrestin(N7T, N308S). As expected, Venus-mPrestin(N7T, N308S, Y667Q) accumulated at the Golgi apparatus, and its plasma membrane/cytoplasm intensity ratio decreased significantly (p = 1.02 × 10^{-7}; Figure 3a,b). The mislocalization of Venus-mPrestin(N7T, N308S, Y667Q) to the Golgi apparatus impaired its ultrasound-sensing ability (p = 0.032; Figure 3c), confirming that plasma-membrane targeting of Venus-mPrestin(N7T, N308S) is required for its response to ultrasound.

Venus-mPrestin(N7T, N308S) was not evenly distributed in the plasma membrane but was concentrated in punctate regions (Figures 1b and 3a). HEK293T cells expressing mPrestin(N7T, N308S) exhibit a significantly higher number of puncta than cells expressing wild-type mPrestin (p = 0.015; Figure S6a). Mislocation of mPrestin(N7T, N308S, Y667Q) at Golgi reduces the number of puncta suggesting that puncta formation of mPrestin requires its plasma membrane targeting (p = 0.032; Figure S6a). We also measured the size of mPrestin(N7T, N308S) puncta in cells. The multiple z-stack images of cells expressing mPrestin(N7T, N308S) were acquired and processed by deconvolution. We then built up the 3-dimensional puncta images by maximal intensity projection and measured their sizes. Quantification data show that the area of mPrestin(N7T, N308S) puncta is 132 ± 6.28 nm^2 (mean ± s.e.m.; Figure S6b). Prestin self-assembles into oligomers to form bullet-shaped complexes in the plasma membrane.[32,33] To evaluate whether self-association of prestin occurred in these punctate regions, we used fluorescence resonance energy transfer (FRET) to examine the oligomerization of Venus- and CFP-tagged mPrestin constructs. A greater FRET efficiency was obtained in the punctate regions of cells expressing mPrestin(N7T, N308S) as compared with cells transfected with mPrestinWT (p = 0.025; Figure S6c,d), indicating that self-association of mPrestin(N7T, N308S) but not mPrestinWT occurred in the punctate regions. Immunofluorescence staining also showed that mPrestin(N7T, N308S) puncta associated with actin filaments and microtubules (Figure S6e). Next, ultrafast imaging of cells transfected with Venus-mPrestin(N7T, N308S) (imaging interval, 17 ms) was used to observe the real-time behavior of Venus-mPrestin(N7T, N308S) puncta upon FUS stimulation. Live-cell imaging and quantification showed that Venus-mPrestin(N7T, N308S) puncta oscillated continuously for a few seconds after being exposed to pulsed 0.5 MHz FUS (Figure 3d,e; Movie S2). Because several waves of calcium responses were observed after a single FUS pulse in the Venus-mPrestin(N7T, N308S)-transfected cells (Figure 1c), we hypothesized that a short pulse of FUS induced sustained oscillation of Venus-mPrestin(N7T, N308S)-positive puncta that then trigger the calcium response for a few seconds. To address this hypothesis, we found that cellular expression of Venus-mPrestin(N7T, N308S, V499G, Y501H), which prevents the electromotility of prestin without affecting its localization to the plasma membrane,[34] blocked oscillation

DOI: 10.1021/acs.nanolett.9b04373
Nano Lett. 2020, 20, 1089−1100

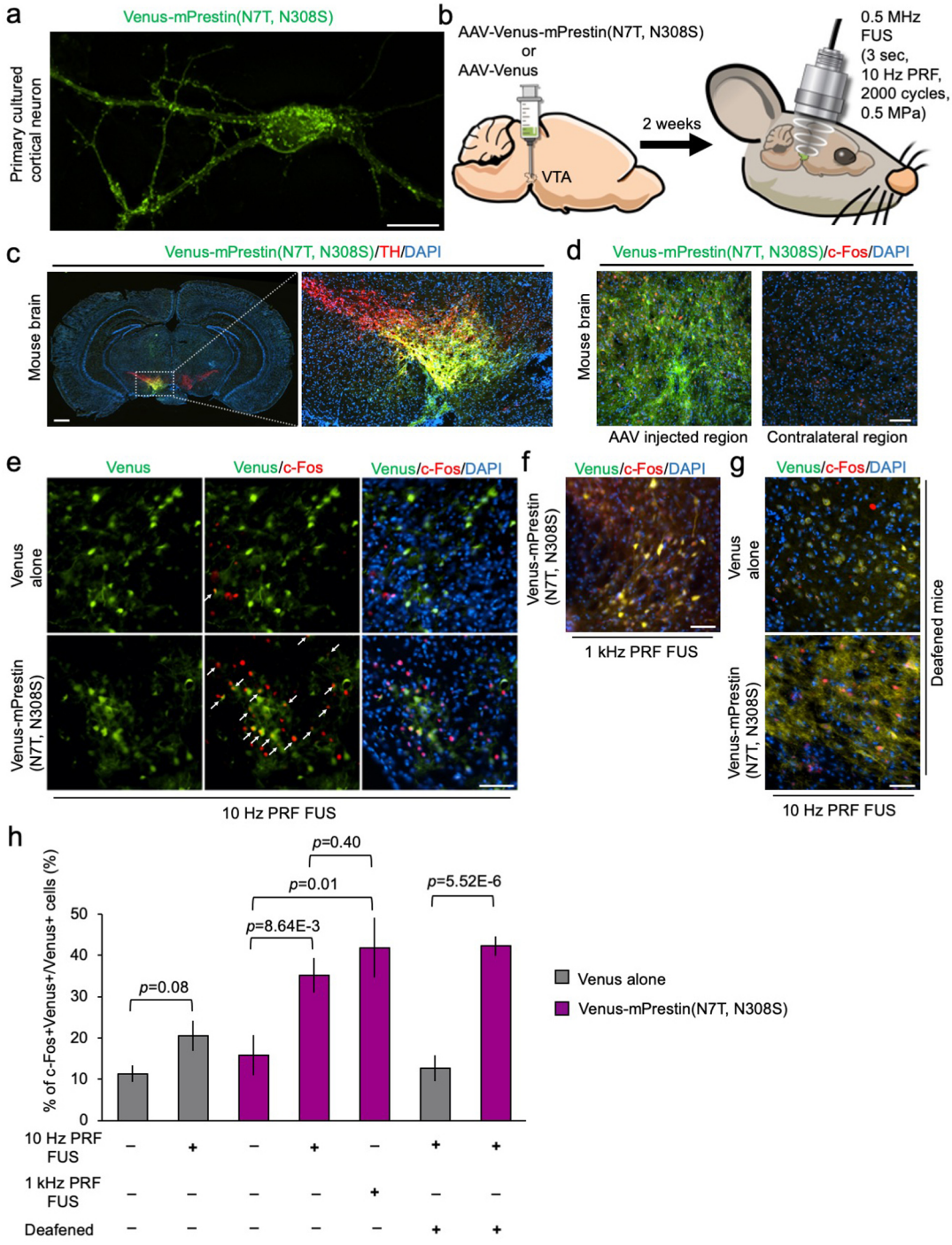

Figure 4. Transcranial FUS stimulation of VTA neurons in mouse brains via mPrestin(N7T, N308S) expression. (a) Representative image of primary cultured cortical neurons expressing Venus-mPrestin(N7T, N308S). The maximum *z*-projection was created from 15 stacks, each separated by 0.3 μm. Scale bar, 20 μm. (b) *In vivo* experimental scheme for transcranial FUS stimulation of the VTA neurons in anesthetized mice. (c) Representative images of mouse brain sections after unilateral injection of AAV-encoding Venus-mPrestin(N7T, N308S) in the TH (tyrosine hydroxylase) positive-VTA region. Scale bar, 1 mm. (d, e) Representative images of mouse brain sections with different conditions. Extensive FUS-driven c-Fos (red) expression was detected in cells expressing Venus-mPrestin(N7T, N308S) after FUS stimulation (0.5 MHz, 0.5 MPa, 10 Hz PRF, 2000 cycles, 3 s duration). Arrows indicate c-Fos+Venus+ cells. Scale bar, 100 μm. (f) Representative image of VTA neurons expressing Venus-mPrestin(N7T, N308S) (yellow) after 1 kHz PRF FUS stimulation (0.5 MHz, 0.5 MPa, 1 kHz PRF, 150 cycles, 6 s duration). Extensive FUS-driven c-Fos (red) expression was detected under this condition. Scale bar, 50 μm. (g) Representative images of VTA neurons expressing Venus alone or Venus-mPrestin(N7T, N308S) (yellow) in chemically deafened mice after 10 Hz PRF FUS stimulation (0.5 MHz, 0.5 MPa, 10 Hz PRF, 2000 cycles, 3 s duration). Extensive FUS-driven c-Fos (red) expression was detected in Venus-mPrestin(N7T, N308S)-transfected cells of chemically deafened mice. Scale bar, 50 μm. (h) Percentage of c-Fos-positive neurons expressing Venus alone or Venus-mPrestin(N7T, N308S) under the different conditions presented in parts e–g. Data are shown as the mean ± s.e.m. for 5–9 different sections from 3 mice per condition.

DOI: 10.1021/acs.nanolett.9b04373
Nano Lett. 2020, 20, 1089–1100

of the puncta upon FUS stimulation (Figure 3d,e; Movie S2). Moreover, the lack of oscillation found for the Venus-mPrestin(N7T, N308S, V499G, Y501H) puncta significantly attenuated the FUS-mediated calcium response (p = 0.016; Figure 3c). Thus, FUS-evoked calcium responses are highly dependent on the electromotility and oscillation of prestin puncta in the plasma membrane.

We next determined in which cellular compartment the calcium is stored that is released by Venus-mPrestin(N7T, N308S) upon FUS stimulation. Addition of the calcium chelator ethylene glycol tetraacetic acid (EGTA) in the extracellular space completely inhibited the calcium response in cells expressing Venus-mPrestin(N7T, N308S) upon ultrasound stimulation ($p = 6.2 \times 10^{-7}$; Figure 3f). However, depletion of the intracellular calcium store by thapsigargin did not significantly affect the ultrasound-mediated calcium response (p = 0.16; Figure 3f). Thus, mPrestin(NT7, N308S) induced calcium influx from the extracellular space instead of from the intracellular calcium pool after FUS excitation. We speculate that replacement of Asn with Thr and Ser at positions 7 and 308, respectively, in mPrestin enhanced its localization to the plasma membrane where its oscillations promoted calcium influx from the extracellular space.

Several mechanosensitive ion channels are activated by high-frequency ultrasound.[20,21] We incubated gentamicin, a pharmaceutical inhibitor of mechanosensitive ion channels,[35] with cells that expressed Venus-mPrestin(N7T, N308S) and found that this treatment did not significantly affect the calcium response upon ultrasound excitation (p = 0.27; Figure 3f). Thus, gentamicin-sensitive ion channels were not involved in the mPrestin(N7T, N308S)-mediated calcium response, which is consistent with results from an ultrasound-inducible system driven by piezoelectric nanoparticles.[28] Ultrasound excites neuronal cells by activating voltage-gated ion channels.[6] To examine the possible involvement of voltage-gated ion channels in our system, cells expressing Venus-mPrestin(N7T, N308S) were incubated with tetrodotoxin (TTX), an inhibitor of voltage-gated ion channels, and then stimulated with 0.5 MHz FUS. However, the percentage of ultrasound-excitable cells transfected with mPrestin(N7T, N308S) was not affected by TTX treatment, indicating that voltage-gated ion channels are not involved in the mPrestin-mediated pathway (p = 0.80; Figure 3f).

To take advantage of the enhanced sensitivity of Venus-mPrestin(N7T, N308S) to ultrasound stimulation, we next developed a sonogenetic system that would allow for stimulating neurons. Infection of primary cultured cortical neurons with a Venus-mPrestin(N7T, N308S)-containing lentivirus led to the expression of Venus-mPrestin(N7T, N308S) on the neuronal membrane. Moreover, Venus-mPrestin(N7T, N308S) also forms puncta on the neuronal membrane (Figure 4a). For the sonogenetic stimulation of target neurons in deep brain, an adeno-associated virus (AAV) encoding Venus-mPrestin(N7T, N308S) was injected into a single side of the VTA brain region (Figure 4b,c). Two weeks later, anesthetized mice were exposed to transcranial pulsed ultrasonic excitation (0.5 MHz FUS, 0.5 MPa, 10 Hz PRF, 3 s duration; Figure 4d). The Venus-mPrestin(N7T, N308S) expression was detected mainly in TH (tyrosine hydroxylase)-positive VTA neurons (46 ± 5.76%) and rarely in VGluT2-positive glutamatergic neurons (6 ± 1.81%) (Figure 4c and Figure S7). FUS-activated neurons were mapped by imaging the expression of c-Fos. Neuronal excitation was triggered by a short pulsed FUS in one hemisphere of the VTA neurons expressing Venus-mPrestin(N7T, N308S)-transfected mice but not in the contralateral region without Venus-mPrestin(N7T, N308S) expression (Figure 4d). A significant increase of c-Fos-positive neurons was also observed after FUS stimulation in the presence of Venus-mPrestin(N7T, N308S) expression ($p = 8.64 \times 10^{-3}$, Figure 4e,h). Although the focal diameter of 0.5 MHz FUS (4.4 mm; Figure S2) is larger than VTA, our ultrasound stimulation did not significantly activate neighboring neurons in the absence of mPrestin(N7T, N308S) expression (Figure 4d and Figure S8). Control mice with Venus alone expression showed no significant increase in c-Fos expression in the VTA region (p = 0.08, Figure 4e,h). Moreover, our ultrasound stimulation did not activate microglia in illuminated sites suggesting that our stimulation does not damage mouse brains (Figure S9).

Several previous studies found that low-frequency transcranial ultrasound (0.2−0.5 MHz) at high PRF (1−1.5 kHz PRF) efficiently activates cortical neurons via the auditory mechanism in mice and guinea pigs.[7,36,37] The parameters of ultrasound (0.5 MHz, 0.5 MPa, 10 Hz PRF, 3 s duration) we used to activate mPrestin(N7T, N308S)-transfected cells did not increase c-Fos expression in auditory regions of mice which is consistent with the previous observation that short PRF ultrasound (<100 Hz PRF) can not activate mouse brains (Figure S10).[7] The high PRF (1 kHz PRF) and longer duration (6 s) of ultrasound (0.5 MHz, 0.5 MPa, 1 kHz PRF, 6 s duration) robustly activate both auditory regions and VTA neurons expressing mPrestin(N7T, N308S) (Figure 4f and Figure S10). However, this parameter of ultrasound only slightly improved the success rates of neuromodulation compared to 10 Hz PRF ultrasound (p = 0.40; Figure 4h). To further verify that the mPrestin(N7T, N308S)-mediated neuromodulation is not dependent on the auditory mechanism, we tried to use 10 Hz PRF ultrasound to activate mPrestin(N7T, N308S)-transfected VTA neurons in chemically deafened mice. The extensive c-Fos expression in cells expressing mPrestin(N7T, N308S) can be observed in deafened mice indicating that this event is not dependent on the auditory mechanism (Figure 4g,h). These results confirmed that low PRF ultrasound (10 Hz PRF) can specifically and directly activate mPrestin(N7T, N308S)-transfected cells but not nontransfected cells in mouse deep brains.

In summary, we here introduced two evolutionarily conserved amino acid substitutions N7T and N308S into mouse prestin which enhances its self-association as well as puncta formation in the plasma membrane (Figures 1 and 3, and Figure S6). These mPrestin(N7T, N308S) puncta highly associate with actin filaments and microtubules in cells (Figure S6e). A short pulse of 0.5 MHz FUS induces sustained oscillation of mPrestin(N7T, N308S) puncta with electromotility and evokes several waves of calcium responses in transfected cells (Figures 1c and 3c−e). The ultrahigh ultrasound sensitivity of mPrestin(N7T, N308S) allows for noninvasive stimulation of target neurons in deep mouse brains by a short pulsed FUS (Figure 4).

Our results have raised a fundamental question: how does 0.5 MHz FUS evoke calcium influx in cells expressing mPrestin(N7T, N308S)? Our ultrasound excitation does not affect temperature *in vitro* and *in vivo* which excludes the scenario that ultrasound activates Prestin via a thermal effect (Figure S11). Several studies have shown that 0.25−0.5 MHz

DOI: 10.1021/acs.nanolett.9b04373
Nano Lett. 2020, 20, 1089−1100

ultrasound waves induce temporal cavitation between two lipid leaflets of the plasma membrane which changes membrane thickness or the membrane potential.[7,38,39] NT and NS mutants lead the prestin target to the plasma membrane where their electromotility nature senses the change of membrane potential and triggers the observed calcium influx (Figure 3c−e). Calcium is known to further enhance the electromotility of prestin,[40] which may act as a positive feedback loop to substantially amplify the ultrasound-induced bioeffects and produce multiple waves of calcium influx (Figure 1c and Figure S12). Ultrasound of 80 kHz, which is the peak frequency used by most sonar species,[23] did not efficiently induce a calcium response in Venus-mPrestin(N7T, N308S)-transfected cells (Figure 2), suggesting that the mechanism(s) of how sonar-responsive species hear ultrasound by auditory organs may not be the same as what mPrestin-(N7T, N308S) dose in nonauditory systems.

Similar to photon-responsive proteins and fluorescent proteins, which absorb distinct wavelengths of light and allow for multiplex imaging and optogenetics, mPrestin(N7T, N308S) specifically responds to 0.5 MHz FUS, suggesting that a multiple-frequency system using ultrasound of 1−15 MHz can be developed to noninvasively diagnose regions of abnormal tissues and simultaneously manipulate cellular activities with 0.5 MHz FUS. Moreover, since 0.5 MHz FUS waves cannot be delivered through the air and are rarely used by sonar species, the natural background level for this frequency is expected to be low. Previously developed simulations and experimental data suggest that ultrasound wavelengths of ∼0.60−0.70 MHz would be optimal for transcranial transmission and brain absorption,[41,42] supporting that our sonogenetic system is a promising tool for therapeutic applications involving the brain. Indeed, our *in vivo* results showed that 0.5 MHz FUS efficiently accesses to the deep brain regions like VTA and stimulates target neurons expressing Venus-mPrestin(N7T, N308S) (Figure 4c−h).

To our knowledge, this mPrestin(N7T, N308S)-based sonogenetic approach is the first system that enables the use of low-frequency ultrasound to efficiently manipulate molecular activities in mammalian cells that are genetically modified. Although heterologous expression of mPrestin(N7T, N308S) significantly enhanced the ultrasound sensitivity of HEK293T cells, the percentage of ultrasound-excitable cells in our system needs improvement. A more detailed understanding of how mPrestin(N7T, N308S) sense and amplify ultrasound waves is needed to engineer different prestin variants that are more sensitive to ultrasound. With ongoing development, engineered ultrasound-responsive proteins and sonogenetic systems should become versatile and powerful tools for noninvasively and precisely manipulating activities of genetically modified cells.

Methodology. *Cell Culture, Chemical Reagents, DNA Constructs, and Transfection.* Human HEK293T cells were cultured in Dulbecco's modified Eagle's medium (DMEM; Gibco) supplemented with 10% (v/v) fetal bovine serum, 5 U/mL penicillin, and 50 μg/mL streptomycin (Gibco). The following Venus- or CFP-tagged mPrestin mutant genes were generated by site-directed mutagenesis: N7T, N308S, Y667Q, V449G, and Y501H. Y667Q and V449G/Y501H are mutants that caused the mislocation and defect of electromotility to prestin, respectively. To construct the pLenti-hSyn1-Venus and pLenti-hSyn1-Venus-mPrestin(N7T, N308S), Q5 high-fidelity DNA polymerase (New England Biolabs) and HiFi assembly kit (New England Biolabs) were used. The hSyn1-Venus and hSyn1-Venus-mPrestin(N7T, N308S) inserts were PCR amplified from hSyn1-Venus-mPrestin(N7T, N308S) construct. The pLenti-backbone and the inset with a molar ratio of 1:2 (backbone:fragment) were HiFi assembled to acquire the corresponding lentiviral vectors. For DNA transfection, LT-1 (Mirus) was used according to the manufacturer's protocol. For inhibitor experiments, gentamicin (200 μM, 20 min, Sigma), TTX (500 nM, 20 min, Abcam), EGTA (5 mM, 20 min, Sigma), and thapsigargin (100 nM, 30 min, Sigma) were used. Before ultrasound excitation, HEK 293T cells were incubated with one of the various inhibitors or 0.1% (v/v) DMSO dissolved in DMEM (Gibco) at 37 °C. Calcium-free, serum-free medium (Gibco) was used in the EGTA experiment.

Live-Cell Imaging. Transfected cells were seeded into Lab-Tek eight-well chambers (Thermo Scientific) coated with poly-D-lysine (P6407, Sigma-Aldrich) or onto 25 mm cover glasses in six-well culture plates (SPL Life Science) that were similarly coated. Live-cell imaging was conducted using a Nikon T1 inverted fluorescence microscope (Nikon) with a 20× or 60× oil objective (Nikon), a DS-Qi2 CMOS camera (Nikon), and Nikon element AR software (Nikon). The cells were held under a 5% CO_2 atmosphere at 37 °C in an environmental chamber (Live Cell Instrument). The distribution of Venus-mPrestinWT, Venus-mPrestin(N7T, N308S), Venus-mPrestin(N7T, N308S, Y667Q), and Venus-mPrestin(N7T, N308S, V499G, Y501H) in HEK293T cells was observed using a Nikon A1 confocal system with a 100× oil objective (Nikon). Multiple *z*-stack images (0.3 μm between stacks; 15 stacks) were acquired and processed with Huygens deconvolution (Scientific Volume Imaging), and the maximum intensity projections of the images were generated by Nikon element AR software. The plasma membrane/cytoplasm intensity ratios of the Venus-mPrestin constructs were analyzed by Nikon element AR software. Ultrafast imaging was acquired under a Nikon A1 confocal system with a Resonant scanner (Nikon) and 100× objective (Nikon).

Calibration of Acoustic Peak Negative Pressure and Power Density of FUS. For the acoustic peak negative pressure measurement, we have recorded voltage traces produced by FUS pressure waves via a calibrated polyvinylidene difluoride type hydrophone (model HGL-0085, ONDA, Sunnyvale, CA; calibration range = 0.25−20 MHz; spatial resolution, 85 μm) and an oscilloscope (LT354, LeCory Co., Chestnut Ridge, NY). Using measurements recorded from hydrophones, the acoustic peak negative pressure then could be calculated by the formula provided on the data sheet. For the acoustic power density measurement, a calibrated ultrasound power meter (Model UPM-DP-1AV, Ohmic Instruments Inc.) was used to detect the power of each FUS stimulus waveform with 30% of duty cycle. The measurements were conducted in an acrylic water tank that was filled with distilled and degassed water at 25 °C.

Immunofluorescence Staining. HEK293T cells transfected with Venus-mPrestin(N7T, N308S) were seeded on poly-D-lysine-coated Lab-Tek eight-well chambers (Thermo Scientific). Transfected cells were fixed with 4% paraformaldehyde (Electron Microscopy Sciences) at room temperature for 15 min and subsequently permeabilized by 0.1% Triton X-100 (Sigma-Aldrich). After incubation of blocking solution (PBS with 2% bovine serum albumin) for 30 min at room temperature, cells were stained with phalloidin Alexa Fluor

DOI: 10.1021/acs.nanolett.9b04373
Nano Lett. 2020, 20, 1089−1100

594 (1:100 dilution; Thermo Scientific, A12381) or anti-α-tubulin antibody (1:1000 dilution; Sigma-Aldrich, T6199) for 1 h at room temperature. Goat antimouse IgG Alexa Fluor 594 (1:1000 dilution; Thermo Scientific, R37121) was incubated with cells for 1 h at room temperature.

In Vitro FUS Stimulation. FUS stimulation (acoustic peak negative pressure, 0.5 MPa; 2000 cycles; PRF, 10 Hz; and 3 s duration) was applied using a single-element FUS transducer (80 kHz FUS: Pro-Wave Electronic Corp.; 0.5, 1, 2, and 3.5 MHz FUS: Panametrics). The ultrasound transducer was driven by a function generator (AFG3251, Tektronix) and a radio frequency power amplifier (80 kHz FUS: 150A100B, AR; 0.5 MHz, 1 MHz, 2 MHz, 3.5 MHz FUS: 325LA, Electronics & Innovation) to transmit the ultrasound pulses. A water cone filled with degassed water was attached to the ultrasound transducer assembly, after which the surface of the cone was submerged into the culture-dish medium. Before starting each experiment, we used a glass bottom dish which was embedded with two acoustically transparent 200 μm diameter vessel-mimicking cellulose tubes in cross shape. The cross point of the two tubes was positioned at the center of the dish (0.5 cm above the bottom). The projection of the tubes' cross point to the dish bottom was also marked onto the glass by a color pen. For aligning the focus of the ultrasound transducer and optical objective, the location of the holder was first appropriately adjusted for ensuring that the marker appeared at the center of the objective. Second, operating the ultrasound transducer in a pulse echo mode and positioning the location of the ultrasound transducer ensured that the focal area of the ultrasound pulse was sonicated at the cross point of the two tubes. Third, the location of the ultrasound transducer was moved down 0.5 cm. Finally, the successful confocal positioned between optical and acoustic foci was verified by injecting microbubbles in the cellulose tube and observing the occurrence of microbubble destruction by ultrasound. To record the calcium influx in a cell in real time, the ultrasound transducer was confocally positioned with the objective of the microscope.

Cell Viability Test. The effect of ultrasound excitation on cell viability was determined by the CCK-8 cell counting kit (Dojindo Laboratories) according to the manufacturer's instructions. In brief, 6×10^5 293T stably expressing Venus alone and Venus-mPrestin(N7T, N308S) were seeded in a 3 cm culture dish, respectively. After overnight incubation at 37 °C, FUS stimulation (acoustic peak negative pressure, 0.5 MPa; 2000 cycles; 10 Hz PRF; and 3 s duration) was applied to cells. At 24 h after FUS stimulation, the cell viability was determined by measuring the optical density of CCK-8 at 450 nm.

Lentivirus Production. Five hours prior to transfection, culture medium of HEK293T cells grown to a confluency of 60% was replaced with 10 mL of DMEM supplemented with GlutaMAX (Gibco, Taipei, Taiwan) and 10% FBS (Hyclone, Taipei, Taiwan) containing 25 μM chloroquine diphosphate (Tokyo Chemical Industry, Taipei, Taiwan). HEK293T cells were cotransfected with 1.3 pmol of psPAX2 (gift from Didier Trono; Addgene plasmid 12260), 0.72 pmol of pMD2.G (gift from Didier Trono; Addgene plasmid 12259), and 1.64 pmol of transfer plasmids (pLenti-hSyn1-Venus or pLenti-hSyn1-Venus-mPrestin(N7T, N308S)) by PEI (Alfa Aesar; 1 mg/mL polyethylenimine, linear, MW 25 000) transfection. The ratio of DNA:PEI was 1:3 diluted in 1 mL of OptiMEM (Gibco). Then, 18 h post-transfection, viral medium was replaced with 15 mL of DMEM supplemented with GlutaMAX and 10% FBS; 48 h post-transfection, viral medium was harvested, stored at 4 °C, and replaced with 15 mL of DMEM supplemented with GlutaMAX and 10% FBS. At 72 h post-transfection, viral medium was pooled with the 48 h harvest and centrifuged at 500*g* for 10 min at 4 °C. The viral supernatant was filtered through a 0.45 μm PES filter (Pall, Taipei, Taiwan), snap frozen with liquid nitrogen, and stored at −80 °C.

Primary Neuronal Culture and Lentivirus Transduction. Sprague−Dawley rats were purchased from BioLASCO Taiwan Co., Ltd. Primary cortical neurons were dissociated from dissected cortices of rat embryos (embryonic day 18, E18) and then seeded on poly-L-lysine (Sigma, Saint Louis, MO)-coated bottom-glass dishes (1.2 × 106 cells per dish). On day *in vitro* 0 (DIV0), primary neurons were cultured in minimum essential medium (Invitrogen, Carlsbad, CA) supplemented with 5% fetal bovine serum (Invitrogen), 5% horse serum (Invitrogen), and 0.5 mg/mL penicillin−streptomycin (Invitrogen) under 5% CO_2 condition. Culture medium was changed to Neurobasal medium (Gibco, Grand Island, NY) containing 25 μM glutamate (Sigma), 2% B-27 supplement (Invitrogen), 0.5 mM L-glutamine (Invitrogen), and 50 units/mL antibiotic−antimycotic (AA) (Invitrogen) on DIV1. Cytosine-β-D-arabinofuranoside (AraC, 10 μM) (Invitrogen) was added to neurons on DIV2 to inhibit proliferation of glial cells. On DIV3, medium was changed to Neurobasal medium containing 2% B-27 supplement, 0.5 mM L-glutamine, and 50 units/mL AA. On DIV6, conditional medium was harvested and half-replaced with fresh Neurobasal/glutamine culture medium. Neurons were infected with hSyn1-Venus or hSyn1-Venus-mPrestin(N7T, N308S)-containing lentivirus on DIV7. After overnight incubation at 37 °C, the virus-containing medium was replaced with conditional culture medium mixed with an equal volume of fresh medium. For further maintenance, the medium was half-changed with fresh Neurobasal/glutamine culture medium every 2 days. After lentivirus infection for 7 days, neurons were imaged by a Nikon T1 inverted fluorescence microscope (Nikon).

Adeno-Associated Virus Delivery. The Venus-mPrestin-(N7T, N308S) or Venus alone-containing adeno-associated virus (AAV) were packaged by NTU CVT-LS-AAV core. A total of 1 μL of AAV encoding Venus-mPrestin(N7T, N308S) or Venus alone was transcranially injected into the left ventral tegmental area (VTA; bregma, −3 mm; left, 0.5 mm; depth, 4.2 mm). During the experiment, the animal was anesthetized with 2% isoflurane gas and immobilized on a stereotactic frame. After AAV injection for 2 weeks, the mice were simulated by FUS.

In Vivo Sonogenetic Stimulation of VTA. The AAV transfected mice were randomly divided into four groups: (1) AAV encoding Venus-mPrestin(N7T, N308S) + 0.5 MHz FUS stimulation group (n = 3 mice); (2) AAV encoding Venus-mPrestin(N7T, N308S) without FUS group (n = 3 mice); (3) AAV encoding Venus alone +0.5 MHz FUS stimulation group (n = 3 mice); and (4) AAV encoding Venus alone without ultrasound group (n = 3 mice). The 0.5 MHz sonication was applied transcranially at the left brain with the acoustic pressure of 0.5 MPa, 2000 cycles, and 10 Hz PRF, sonication duration of 3 s and one sonication site. In the experiments of Figure 4f and Figure S10, the parameter of ultrasound with high PRF and longer duration (0.5 MHz, 0.5 MPa, 150 cycles, 1 kHz PRF, 6 s duration) was also used to

DOI: 10.1021/acs.nanolett.9b04373
Nano Lett. 2020, 20, 1089−1100

test its effect on auditory regions of mouse brains and mPrestin(N7T, N308S)-transfected cells. In the deafened animal group, the animals were chemically deafened by injection of kanamycin (1 g/kg, subcutaneous injection) and Furosemide (30 min later, 200 mg/kg, intraperitoneal injection).[37,43] To induce intracerebral hemorrhage (Figure S9), the mice were injected with a self-made lipid-shell microbubble solution (0.7−1.1 μm, 100 μL, 1×10^8 particles/mL) by retro-orbital injection. Then, 20 s later, the FUS (0.5 MHz, 0.5 MPa, 10 Hz PRF, 5000 cycles, 120 s duration) was delivered to the left brains of mice. During the experiment, the animal was anesthetized with 2% isoflurane gas and immobilized on a stereotactic frame.

Immunohistochemistry Staining (IHC) and Quantification of c-Fos Expression. The successful stimulation of mPrestin-(N7T, N308S)-transfected cells was verified by c-Fos IHC staining.[44] The brains of mice were removed at 90 min after 0.5 MHz FUS stimulation. The brains were then sliced into 15 μm sections and incubated into 5% goat serum and PBS for 1 h to block the endogenous proteins. The sections were then incubated in anti-c-Fos antibody (1:1000; SYSY), antityrosine hydroxylase antibody (1:500; Abcam), anti-VGluT2 antibody (1:500; Abcam), or anti-lba1 antibody (1:500; Abcam) in antibody diluent for overnight. The sections were then incubated for 1 h in Dylight 594 conjugated secondary antibody (1:500; GeneTex) in antibody diluent followed by several washes in PBS. The cellular nuclei were labeled by DAPI. Finally, the slides were coverslipped with fluorescent mounting medium and stored flat in the dark at −20 °C. The successful transfection of mPrestin was confirmed by the expression of Venus fluorescent protein. The number of cells with Venus+c-Fos+ cells were counted in regions of interest of 450 μm × 450 μm. Three ROIs were selected from each section and then averaged. For statistics, slices from at least 3 mice were obtained, imaged, and analyzed. Both imaging and analysis were performed blind to the experimental conditions.

Measurement of the Thermal Effect upon Ultrasound Stimulation. A thermocouple probe (HYP-1, Omega engineering Inc., Stamford, CT) was placed onto the culture dish or the VTA region of mouse brains. The change of temperature was measured upon ultrasound stimulation.

■ ASSOCIATED CONTENT

Supporting Information

The Supporting Information is available free of charge at https://pubs.acs.org/doi/10.1021/acs.nanolett.9b04373.

Computer-controlled live-cell imaging and ultrasound-exposure system, calibration of acoustic pressure of ultrasound transducers, cell viability, membrane integrity of cells, weak ultrasound-evoked calcium response, characterization of mPrestin(N7T, N308S)-positive puncta, mPrestin(N7T, N308S) expression, ultrasound stimulation results, FUS stimulation, ultrasound at high pulse repetition frequency, working model, transducer characteristics and operating frequency ranges, and a summary of acoustic peak negative pressure and power density used in this study (PDF)

Movie S1: mPrestin(N7T, N308S) enables an ultrasound-evoked calcium response (MP4)

Movie S2: mPrestin(N7T, N308S)-positive puncta oscillated upon FUS stimulation (MP4)

■ AUTHOR INFORMATION

Corresponding Authors

*E-mail: ckyeh@mx.nthu.edu.tw.
*E-mail: ycl@life.nthu.edu.tw.

ORCID

Chih-Kuang Yeh: 0000-0002-2880-6327
Yu-Chun Lin: 0000-0002-9629-7560

Author Contributions

Y.-S. Huang, C.-H. Fan, and N. Hsu contributed equally to this work. Y.-S. Huang, C.-H. Fan, C.-K. Yeh, and Y.-C. Lin designed the experiments. C.-H. Fan and C.-Y. Wu programmed the ultrasound system, under the supervision of C.-K. Yeh. Y.-S. Huang, Y.-C. Chang, S.-R. Hong, Y.-C. Lin, W.-C. Hsu, B.-H. Wu, and C.-Y. Chang performed the cell biology experiments. Y.-S. Huang, C.-H. Fan, N. Hsu, Y.-C. Chang, and W.-C. Hsu quantified the imaging results. Y.-S. Huang, S.-R. Hong, and Y.-C. Lin generated the DNA constructs. A. Y.-T. Wu designed and cloned the lentiviral plasmid. V. Guo packaged the lentiviruses. C. P.-K. Lai supervised the molecular cloning and lentiviral production processes. C.-Y. Chang prepared the primary cultured cortical neurons under the supervision of L. Chen. C.-H. Fan and N.-H. Chiu performed the animal experiments. C.-H. Fan, C.-K. Yeh, and Y.-C. Lin wrote the paper.

Funding

This study was supported in part by the Ministry of Science and Technology (MOST), Taiwan (MOST grant numbers 105-2221-E-007-055 105-2119-M-182-001, 108-2221-E-007-040-MY3, and 108-2221-E-007-041-MY3 to C.-K. Yeh; 104-2320-B-007-005-MY2 and 106-2320-B-007-004-MY3 to C. P.-K. Lai; 104-2311-B-007-001, 105-2628-B-007-001-MY3, 107-2628-B-007-001, 108-2638-B-010-001-MY2, and 108-2636-B-007-003 to Y.-C. Lin). Additional funding consisted of a grant from the Program for Translational Innovation of Biopharmaceutical Development-Technology Supporting Platform Axis (Grant 107-0210-01-19-04) to Y.-C. Lin; four grants from the National Tsing Hua University (Grants 107Q2705E1, 108Q2717E1, 107Q2703E1, and 108Q2703E1) to Y.-C. Lin, C.-K. Yeh, and L. Chen; a grant from Academia Sinica Innovative Materials and Analysis Technology Exploration (i-MATE) Program (Grant AS-iMATE-107-33) to C. P.-K. Lai; and a grant from National Health Research Institutes (Grant NHRI-EX108-10813NI) to L. Chen.

Notes

The authors declare the following competing financial interest(s): The patents of mPresin(N7T, N308S) and relative sonogenetic tools are pending.

■ ACKNOWLEDGMENTS

We thank Dr. Jian Zuo (St. Jude Children's Research Hospital) for the Venus-mouse PrestinWT construct; Dr. Insuk So (Seoul National University College of Medicine) for hTRPC4α-CFP and mTRPC4β-CFP constructs; and Dr. Takanari Inoue (Johns Hopkins University School of Medicine) for the CFP-R-GECO, R-GECO, mCherry-CAAX, and mCherry-Giantin constructs. Dr. Takanari Inoue (Johns Hopkins University School of Medicine), Dr. Tsung-Han Kuo (National Tsing Hua University), Dr. Hau-Jie Yau (National Taiwan University) are thanked for critical reading of the manuscript.

DOI: 10.1021/acs.nanolett.9b04373
Nano Lett. 2020, 20, 1089−1100

■ ABBREVIATIONS

FUS, focused ultrasound; MBs, gas-filled microbubbles; TTX, tetrodotoxin; EGTA, ethylene glycol tetraacetic acid; AAV, adeno-associated virus; VTA, ventral tegmental area.

■ REFERENCES

(1) Yizhar, O.; Fenno, L. E.; Davidson, T. J.; Mogri, M.; Deisseroth, K. Optogenetics in Neural Systems. *Neuron* **2011**, *71* (1), 9−34.

(2) Sternson, S. M.; Roth, B. L. Chemogenetic Tools to Interrogate Brain Functions. *Annu. Rev. Neurosci.* **2014**, *37*, 387−407.

(3) Qin, S.; Yin, H.; Yang, C.; Dou, Y.; Liu, Z.; Zhang, P.; Yu, H.; Huang, Y.; Feng, J.; Hao, J.; et al. A Magnetic Protein Biocompass. *Nat. Mater.* **2016**, *15* (2), 217−226.

(4) Stanley, S. A.; Sauer, J.; Kane, R. S.; Dordick, J. S.; Friedman, J. M. Remote Regulation of Glucose Homeostasis in Mice Using Genetically Encoded Nanoparticles. *Nat. Med.* **2015**, *21* (1), 92−98.

(5) Maresca, D.; Lakshmanan, A.; Abedi, M.; Bar-Zion, A.; Farhadi, A.; Lu, G. J.; Szablowski, J. O.; Wu, D.; Yoo, S.; Shapiro, M. G. Biomolecular Ultrasound and Sonogenetics. *Annu. Rev. Chem. Biomol. Eng.* **2018**, *9* (1), 229−252.

(6) Tyler, W. J.; Tufail, Y.; Finsterwald, M.; Tauchmann, M. L.; Olson, E. J.; Majestic, C. Remote Excitation of Neuronal Circuits Using Low-Intensity, Low-Frequency Ultrasound. *PLoS One* **2008**, *3* (10), e3511.

(7) King, R. L.; Brown, J. R.; Newsome, W. T.; Pauly, K. B. Effective Parameters for Ultrasound-Induced in Vivo Neurostimulation. *Ultrasound Med. Biol.* **2013**, *39* (2), 312−331.

(8) Tufail, Y.; Matyushov, A.; Baldwin, N.; Tauchmann, M. L.; Georges, J.; Yoshihiro, A.; Tillery, S. I. H.; Tyler, W. J. Transcranial Pulsed Ultrasound Stimulates Intact Brain Circuits. *Neuron* **2010**, *66* (5), 681−694.

(9) Tufail, Y.; Yoshihiro, A.; Pati, S.; Li, M. M.; Tyler, W. J. Ultrasonic Neuromodulation by Brain Stimulation with Transcranial Ultrasound. *Nat. Protoc.* **2011**, *6* (9), 1453−1470.

(10) Yoo, S. S.; Bystritsky, A.; Lee, J. H.; Zhang, Y.; Fischer, K.; Min, B. K.; McDannold, N. J.; Pascual-Leone, A.; Jolesz, F. A. Focused Ultrasound Modulates Region-Specific Brain Activity. *NeuroImage* **2011**, *56* (3), 1267−1275.

(11) Menz, M. D.; Oralkan, O.; Khuri-Yakub, P. T.; Baccus, S. a. Precise Neural Stimulation in the Retina Using Focused Ultrasound. *J. Neurosci.* **2013**, *33* (10), 4550−4560.

(12) Tsui, P. H.; Wang, S. H.; Huang, C. C. In Vitro Effects of Ultrasound with Different Energies on the Conduction Properties of Neural Tissue. *Ultrasonics* **2005**, *43* (7), 560−565.

(13) Foley, J. L. J.; Little, J. W. J. J. W.; Vaezy, S. Image-Guided High-Intensity Focused Ultrasound for Conduction Block of Peripheral Nerves. *Ann. Biomed. Eng.* **2006**, *35* (1), 109−119.

(14) Meijering, B. D. M.; Juffermans, L. J. M.; Van Wamel, A.; Henning, R. H.; Zuhorn, I. S.; Emmer, M.; Versteilen, A. M. G.; Paulus, W. J.; Van Gilst, W. H.; Kooiman, K.; et al. Ultrasound and Microbubble-Targeted Delivery of Macromolecules Is Regulated by Induction of Endocytosis and Pore Formation. *Circ. Res.* **2009**, *104* (5), 679−687.

(15) Fan, Z.; Liu, H.; Mayer, M.; Deng, C. X. Spatiotemporally Controlled Single Cell Sonoporation. *Proc. Natl. Acad. Sci. U. S. A.* **2012**, *109* (41), 16486−16491.

(16) Ibsen, S.; Tong, A.; Schutt, C.; Esener, S.; Chalasani, S. H. Sonogenetics Is a Non-Invasive Approach to Activating Neurons in Caenorhabditis Elegans. *Nat. Commun.* **2015**, *6*, 1−12.

(17) Willmann, J.; Cheng, Z.; Davis, C.; Lutz, A.; Schipper, M.; Nielsen, C.; Gambhir, S. Targeted Microbubbles for Imaging Tumor Angiogenesis : Assessment of Whole-Body Biodistribution with Dynamic Micro-PEI in Mice. *Radiology* **2008**, *249* (1), 212−219.

(18) Lakshmanan, A.; Farhadi, A.; Nety, S. P.; Lee-Gosselin, A.; Bourdeau, R. W.; Maresca, D.; Shapiro, M. G. Molecular Engineering of Acoustic Protein Nanostructures. *ACS Nano* **2016**, *10* (8), 7314−7322.

(19) Bourdeau, R.; Lee-Gosselin, A.; Lakshmanan, A.; Kumar, S.; Farhadi, A.; Shapiro, M. Acoustic Reporter Genes for Non-Invasive Imaging of Microbes in Mammalian Hosts. *Nature* **2018**, *553* (7686), 86−90.

(20) Prieto, M. L.; Firouzi, K.; Khuri-Yakub, B. T.; Maduke, M. Activation of Piezo1 but Not NaV1.2 Channels by Ultrasound at 43 MHz. *Ultrasound Med. Biol.* **2018**, *44* (6), 1217−1232.

(21) Ye, J.; Tang, S.; Meng, L.; Li, X.; Wen, X.; Chen, S.; Niu, L.; Li, X.; Qiu, W.; Hu, H.; et al. Ultrasonic Control of Neural Activity through Activation of the Mechanosensitive Channel MscL. *Nano Lett.* **2018**, *18* (7), 4148−4155.

(22) Fettiplace, R.; Hackney, C. M. The Sensory and Motor Roles of Auditory Hair Cells. *Nat. Rev. Neurosci.* **2006**, *7* (1), 19−29.

(23) Rossiter, S. J.; Zhang, S.; Liu, Y. Prestin and High Frequency Hearing in Mammals. *Commun. Integr. Biol.* **2011**, *4*, 236.

(24) Liu, Z.; Qi, F.-Y.; Zhou, X.; Ren, H.-Q.; Shi, P. Parallel Sites Implicate Functional Convergence of the Hearing Gene Prestin among Echolocating Mammals. *Mol. Biol. Evol.* **2014**, *31* (9), 2415−2424.

(25) Dallos, P.; Fakler, B. Prestin, a New Type of Motor Protein. *Nat. Rev. Mol. Cell Biol.* **2002**, *3* (2), 104−111.

(26) Ludwig, J.; Oliver, D.; Frank, G.; Klöcker, N.; Gummer, A. W.; Fakler, B. Reciprocal Electromechanical Properties of Rat Prestin: The Motor Molecule from Rat Outer Hair Cells. *Proc. Natl. Acad. Sci. U. S. A.* **2001**, *98* (7), 4178−4183.

(27) Pan, Y.; Yoon, S.; Sun, J.; Huang, Z.; Lee, C.; Allen, M.; Wu, Y.; Chang, Y.-J.; Sadelain, M.; Shung, K. K.; et al. Mechanogenetics for the Remote and Noninvasive Control of Cancer Immunotherapy. *Proc. Natl. Acad. Sci. U. S. A.* **2018**, *115* (5), 992−997.

(28) Marino, A.; Arai, S.; Hou, Y.; Sinibaldi, E.; Pellegrino, M.; Chang, Y. T.; Mazzolai, B.; Mattoli, V.; Suzuki, M.; Ciofani, G. Piezoelectric Nanoparticle-Assisted Wireless Neuronal Stimulation. *ACS Nano* **2015**, *9* (7), 7678−7689.

(29) Song, H. B.; Jun, H. O.; Kim, J. H.; Fruttiger, M.; Kim, J. H. Suppression of Transient Receptor Potential Canonical Channel 4 Inhibits Vascular Endothelial Growth Factor-Induced Retinal Neovascularization. *Cell Calcium* **2015**, *57* (2), 101−108.

(30) Myeong, J.; Kwak, M.; Hong, C.; Jeon, J. H.; So, I. Identification of a Membrane-Targeting Domain of the Transient Receptor Potential Canonical (TRPC)4 Channel Unrelated to Its Formation of a Tetrameric Structure. *J. Biol. Chem.* **2014**, *289* (50), 34990−35002.

(31) Zhang, Y.; Moeini-Naghani, I.; Bai, J.; Santos-Sacchi, J.; Navaratnam, D. S. Tyrosine Motifs Are Required for Prestin Basolateral Membrane Targeting. *Biol. Open* **2015**, *4*, 197−205.

(32) Greeson, J. N.; Organ, L. E.; Pereira, F. a.; Raphael, R. M. Assessment of Prestin Self-Association Using Fluorescence Resonance Energy Transfer. *Brain Res.* **2006**, *1091* (1), 140−150.

(33) Mio, K.; Kubo, Y.; Ogura, T.; Yamamoto, T.; Arisaka, F.; Sato, C. The Motor Protein Prestin Is a Bullet-Shaped Molecule with Inner Cavities. *J. Biol. Chem.* **2008**, *283* (2), 1137−1145.

(34) Zheng, J.; Du, G.-G.; Matsuda, K.; Orem, A.; Aguiñaga, S.; Deák, L.; Navarrete, E.; Madison, L. D.; Dallos, P. The C-Terminus of Prestin Influences Nonlinear Capacitance and Plasma Membrane Targeting. *J. Cell Sci.* **2005**, *118* (13), 2987−2996.

(35) Jacques-Fricke, B. T. Ca2+ Influx through Mechanosensitive Channels Inhibits Neurite Outgrowth in Opposition to Other Influx Pathways and Release from Intracellular Stores. *J. Neurosci.* **2006**, *26* (21), 5656−5664.

(36) Guo, H.; Hamilton, M.; Offutt, S. J.; Gloeckner, C. D.; Li, T.; Kim, Y.; Legon, W.; Alford, J. K.; Lim, H. H. Ultrasound Produces Extensive Brain Activation via a Cochlear Pathway. *Neuron* **2018**, *98* (5), 1020−1030e4.

(37) Sato, T.; Shapiro, M. G.; Tsao, D. Y. Ultrasonic Neuromodulation Causes Widespread Cortical Activation via an Indirect Auditory Mechanism. *Neuron* **2018**, *98* (5), 1031−1041e5.

(38) Krasovitski, B.; Frenkel, V.; Shoham, S.; Kimmel, E. Intramembrane Cavitation as a Unifying Mechanism for Ultra-

DOI: 10.1021/acs.nanolett.9b04373
Nano Lett. 2020, 20, 1089−1100

sound-Induced Bioeffects. *Proc. Natl. Acad. Sci. U. S. A.* **2011**, *108* (8), 3258−3263.
(39) Plaksin, M.; Shoham, S.; Kimmel, E. Intramembrane Cavitation as a Predictive Bio-Piezoelectric Mechanism for Ultrasonic Brain Stimulation. *Phys. Rev. X* **2014**, *4* (1), 1−10.
(40) Keller, J. P.; Homma, K.; Duan, C.; Zheng, J.; Cheatham, M. A.; Dallos, P. Functional Regulation of the SLC26-Family Protein Prestin by Calcium/Calmodulin. *J. Neurosci.* **2014**, *34* (4), 1325−1332.
(41) Hayner, M.; Hynynen, K. Numerical Analysis of Ultrasonic Transmission and Absorption of Oblique Plane Waves through the Human Skull. *J. Acoust. Soc. Am.* **2001**, *110* (6), 3319−3330.
(42) White, P. J.; Clement, G. T.; Hynynen, K. Local Frequency Dependence in Transcranial Ultrasound Transmission. *AIP Conf. Proc.* **2005**, *829*, 256−260.
(43) Li, Y.; Ding, D.; Jiang, H.; Fu, Y.; Salvi, R. Co-Administration of Cisplatin and Furosemide Causes Rapid and Massive Loss of Cochlear Hair Cells in Mice. *Neurotoxic. Res.* **2011**, *20* (4), 307−319.
(44) Sundquist, S. J.; Nisenbaum, L. K. Fast Fos: Rapid Protocols for Single- and Double-Labeling c-Fos Immunohistochemistry in Fresh Frozen Brain Sections. *J. Neurosci. Methods* **2005**, *141* (1), 9−20.

DOI: 10.1021/acs.nanolett.9b04373
Nano Lett. 2020, 20, 1089−1100